

Gamma spectroscopy with AGATA: New insights in nuclear excitations along the nuclear chart

- γ -ray tracking
- Physics campaigns
- High energy γ rays & E1 strength
- Isospin symmetrie
- Lifetime measurements
- Outlook

Peter Reiter

Institute of Nuclear Physics, University of Cologne



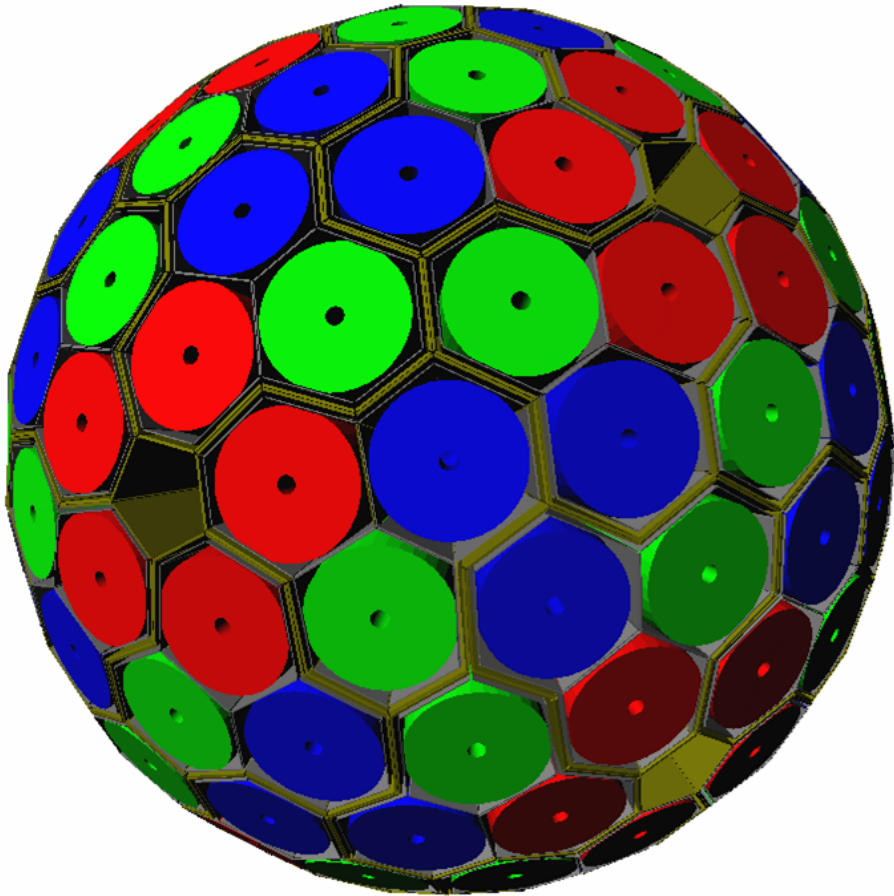
DPG Spring Meeting 2024
Justus-Liebig-Universität Gießen



Advanced GAMMA Tracking Array



13 Countries, 41 Institutions



180 hexagonal HPGe crystals
36-fold segmentation
60 triple-clusters

3 shapes

6480 segments

Solid angle coverage
Inner radius (Ge)

82 %

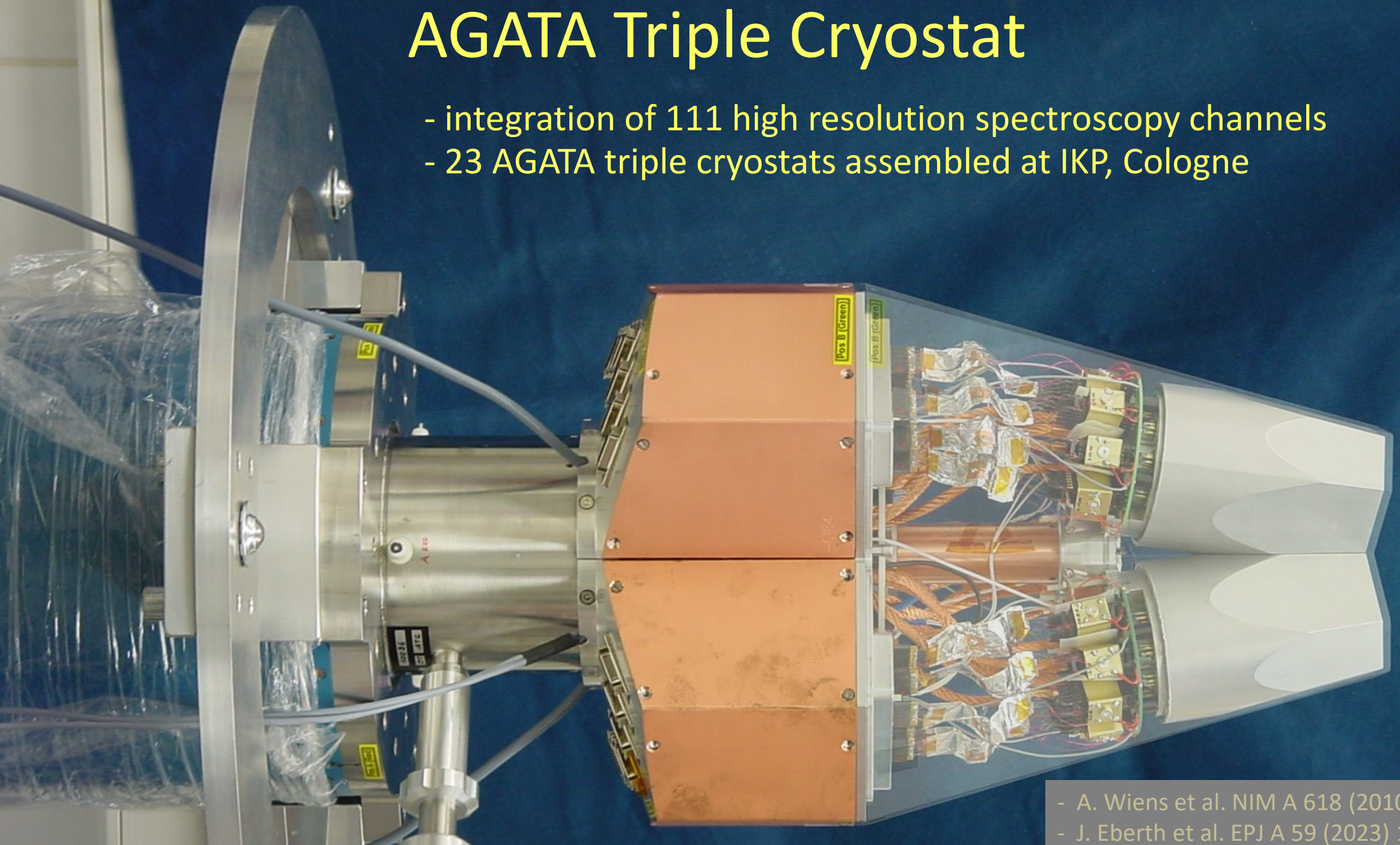
23.5 cm

Efficiency: 43%

Peak/Total: 58%

AGATA Triple Cryostat

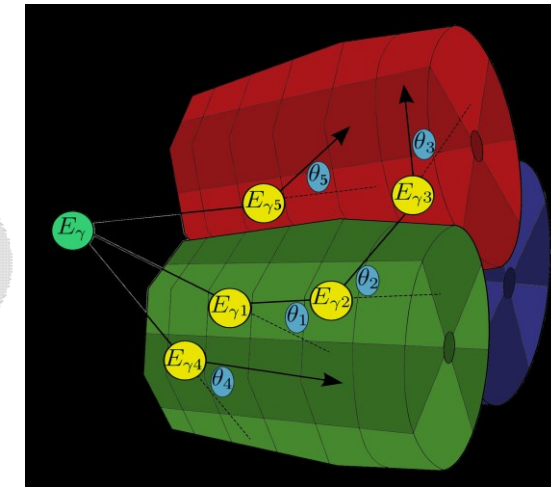
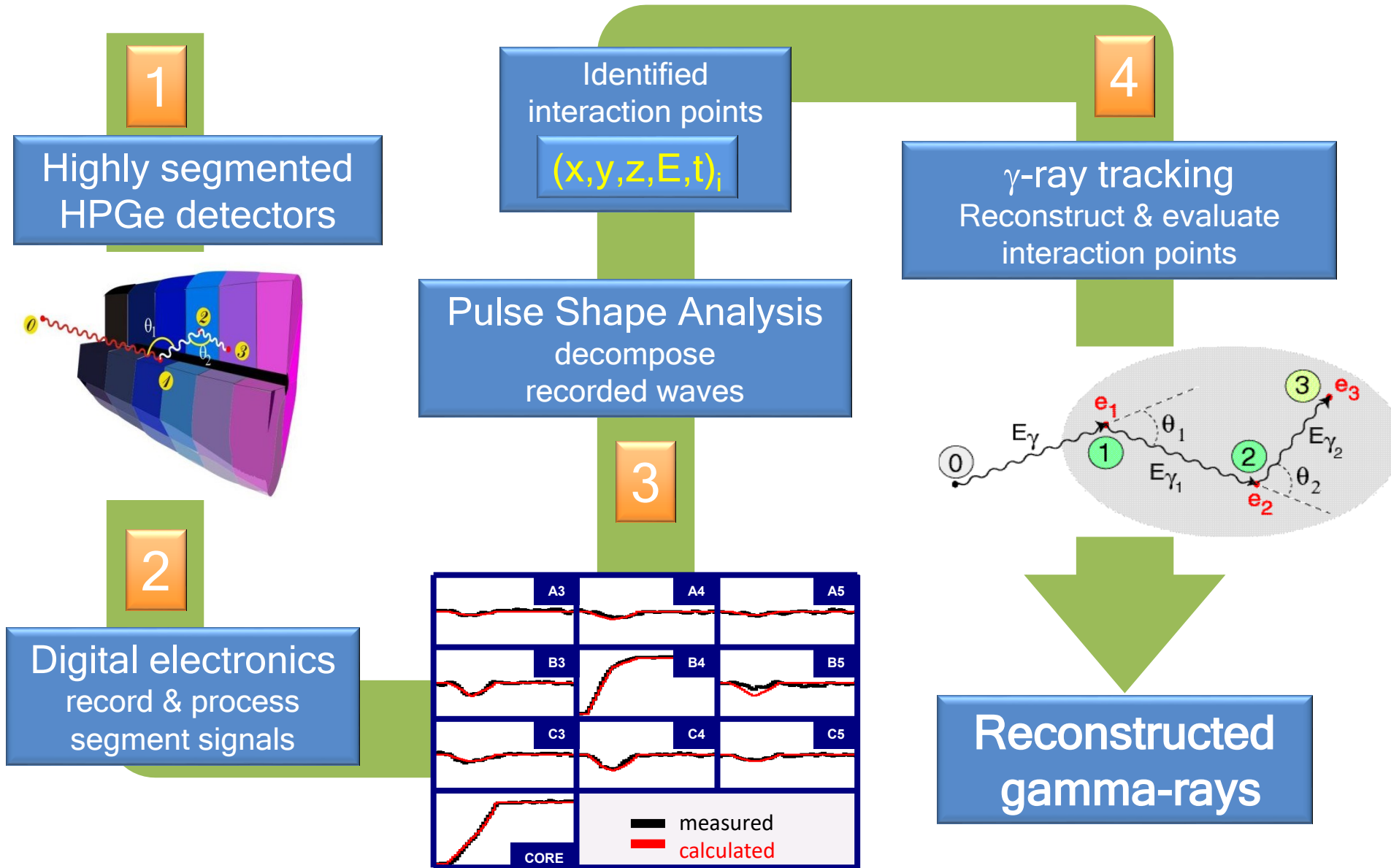
- integration of 111 high resolution spectroscopy channels
- 23 AGATA triple cryostats assembled at IKP, Cologne



- A. Wiens et al. NIM A 618 (2010) 223–233

- J. Eberth et al. EPJ A 59 (2023) 179

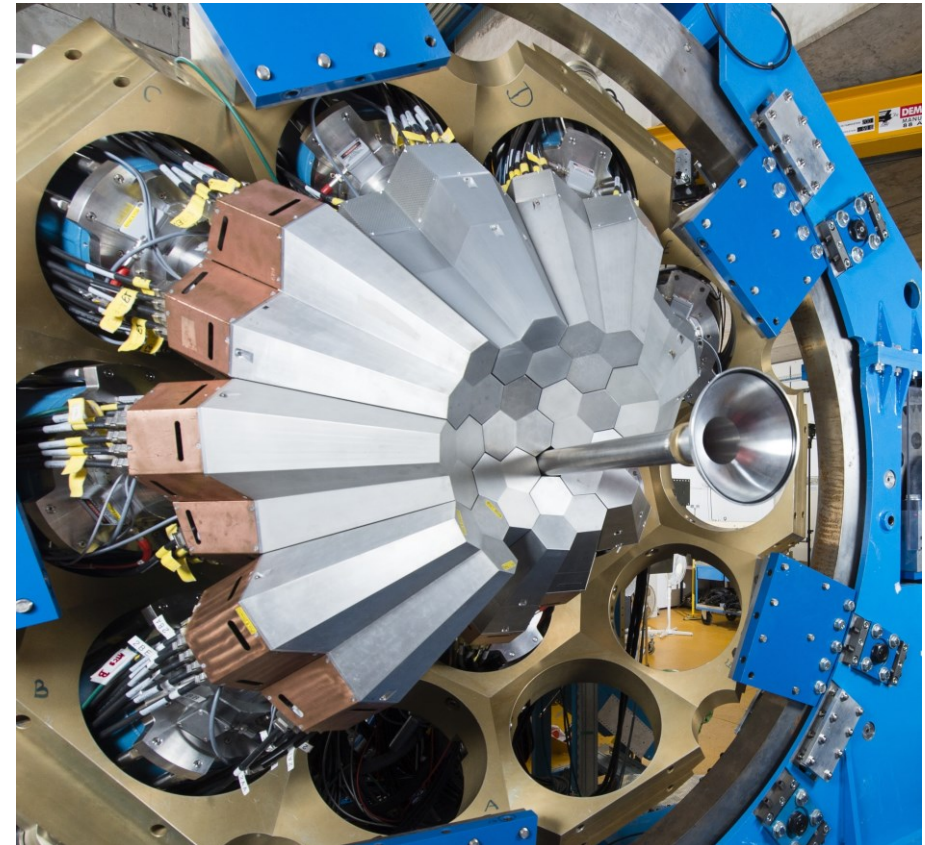
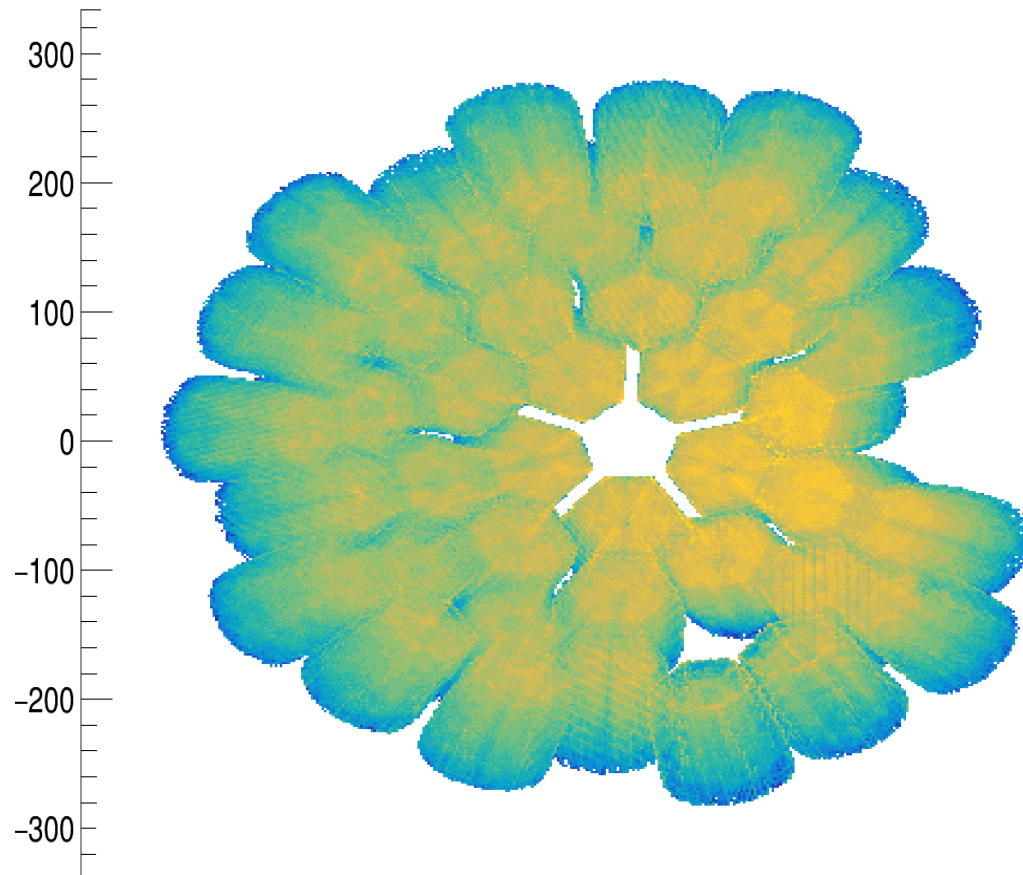
Ingredients of γ -ray tracking



Result of AGATA tracking

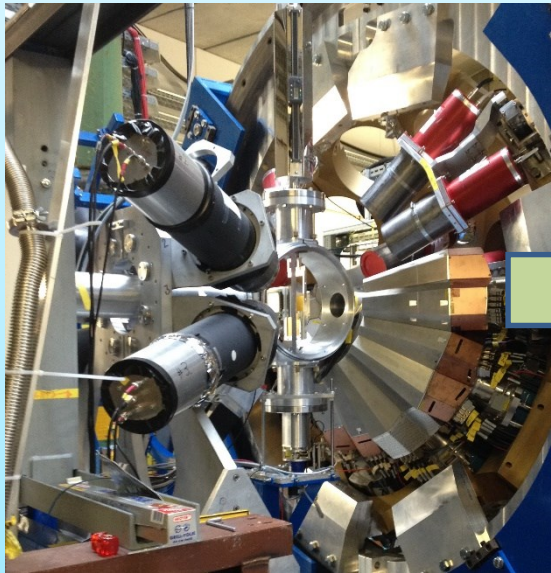
- Reconstructed initial gamma rays with:
- gamma ray energy
 - 1st interaction position → Doppler correction
 - 2nd interaction position → Polarization
 - position resolution < 4 mm FWHM

1st interaction positions
after PSA and Tracking



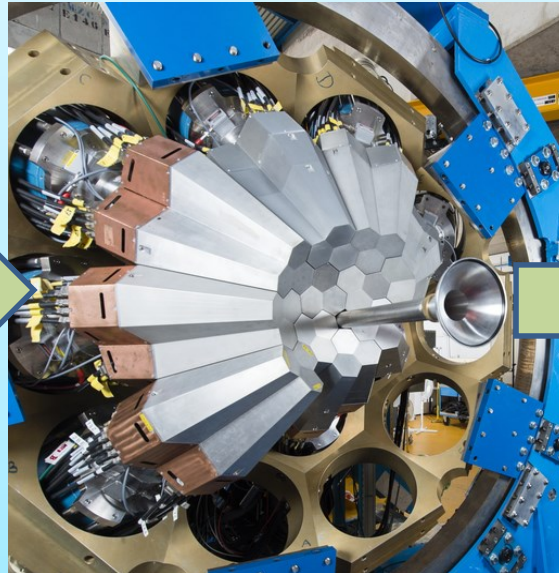
The AGATA journey...

2012-2014
GSI, Germany
25 detectors



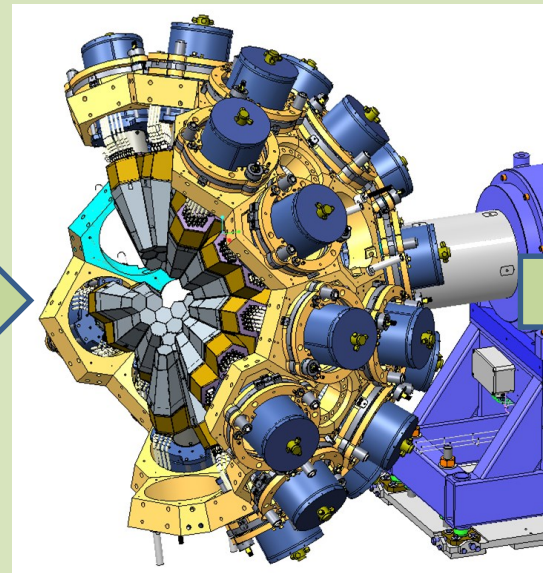
AGATA at GSI

2015-2021
GANIL, France
45 detectors



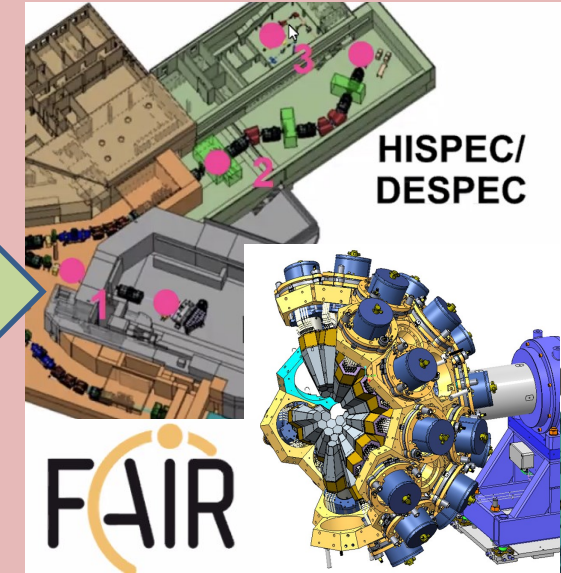
AGATA at GANIL

2021-
Legnaro, Italy
60 detectors



AGATA at LNL

FAIR, Germany
80-90 detectors

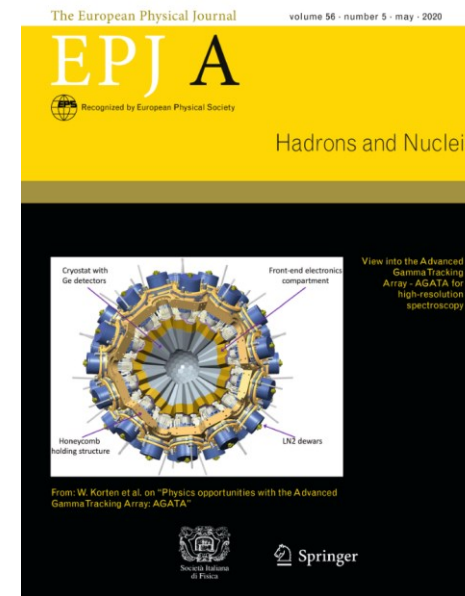
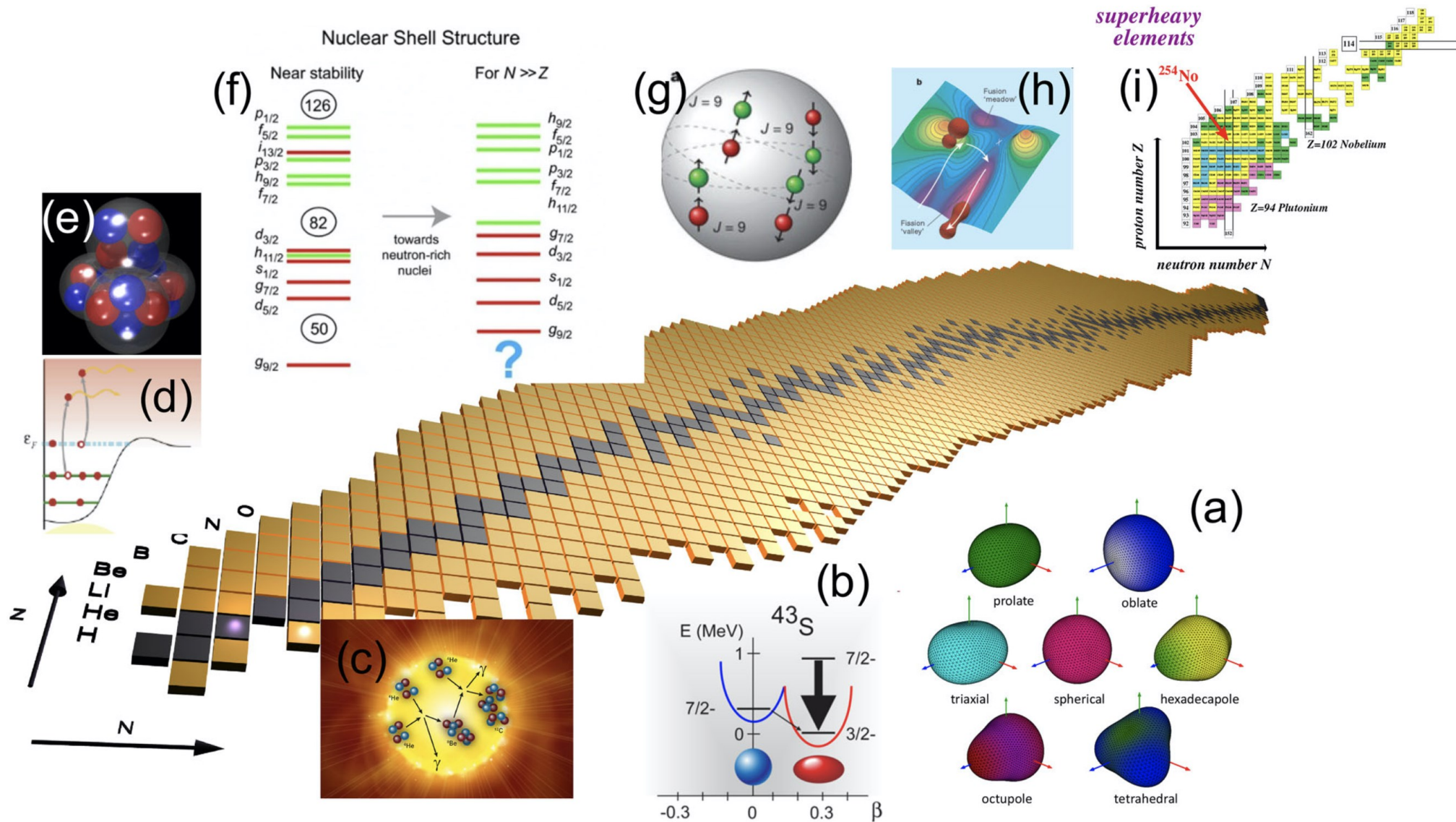


AGATA at NUSTAR

- Coulomb excitation, direct reactions, multi nucleon transfer, deep inelastic, fusion
- **Direct and inverse kinematics**
- $\beta \sim 10\%$
- **Reaccelerated RIBs**

- In-flight RIBs:**
- relativistic Coulomb excitation, knockout, fragmentation.
- $\beta \sim 50\%$

Physics case of AGATA



White book: Physics opportunities with the Advanced Gamma Tracking Array: AGATA



Low energy tail of E1 and E2 response

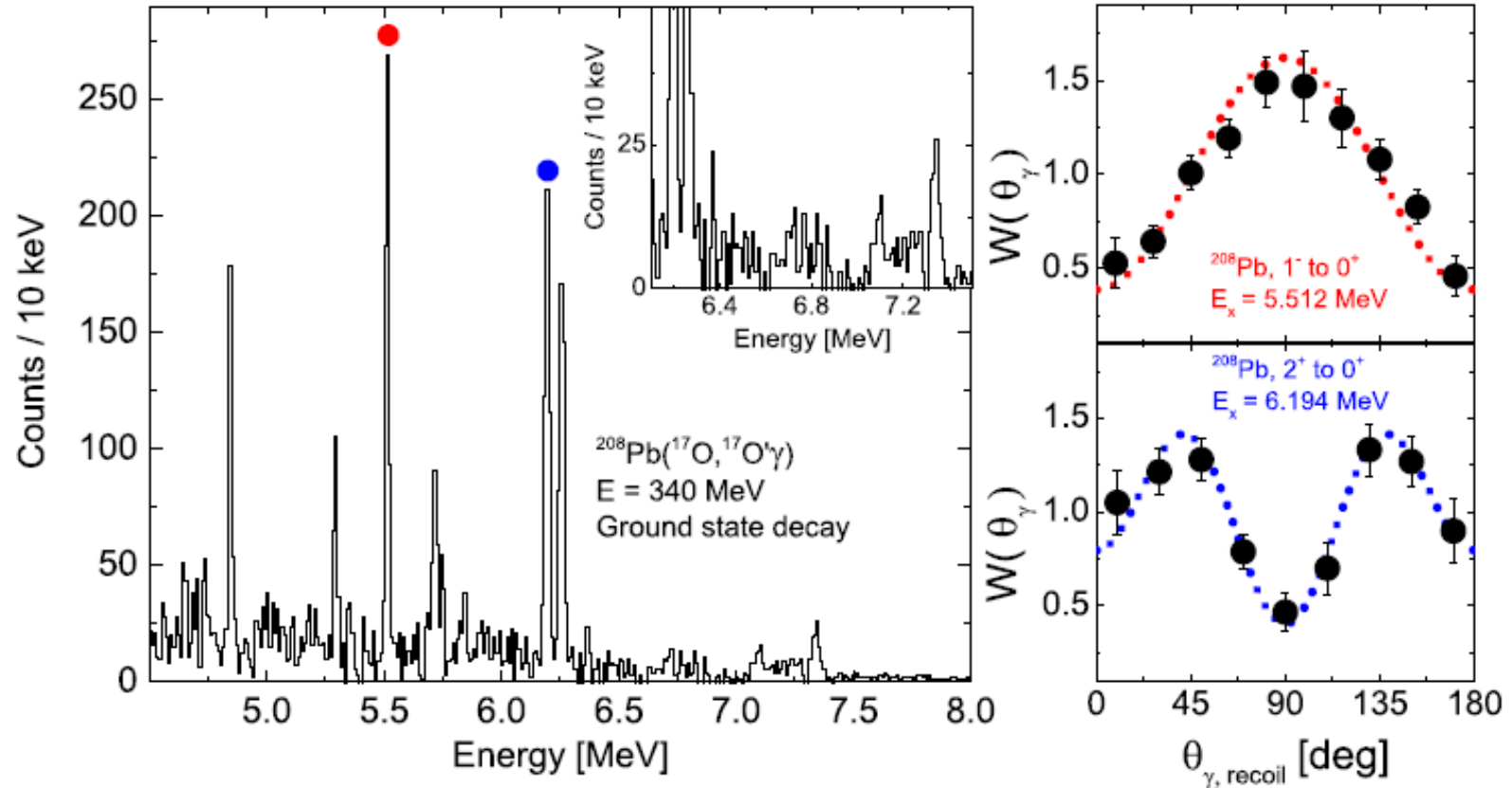
AGATA + ΔE -E Si telescope @ LNL

isoscalar hadronic probe: (^{17}O , $^{17}\text{O}'\gamma$)

targets: ^{90}Zr , ^{124}Sn , ^{140}Ce , ^{208}Pb

investigation of Pygmy dipole resonance
structural splitting of low-lying $E1$ strength

comparison α scattering (α , $\alpha'\gamma$),
photon scattering (γ , γ')

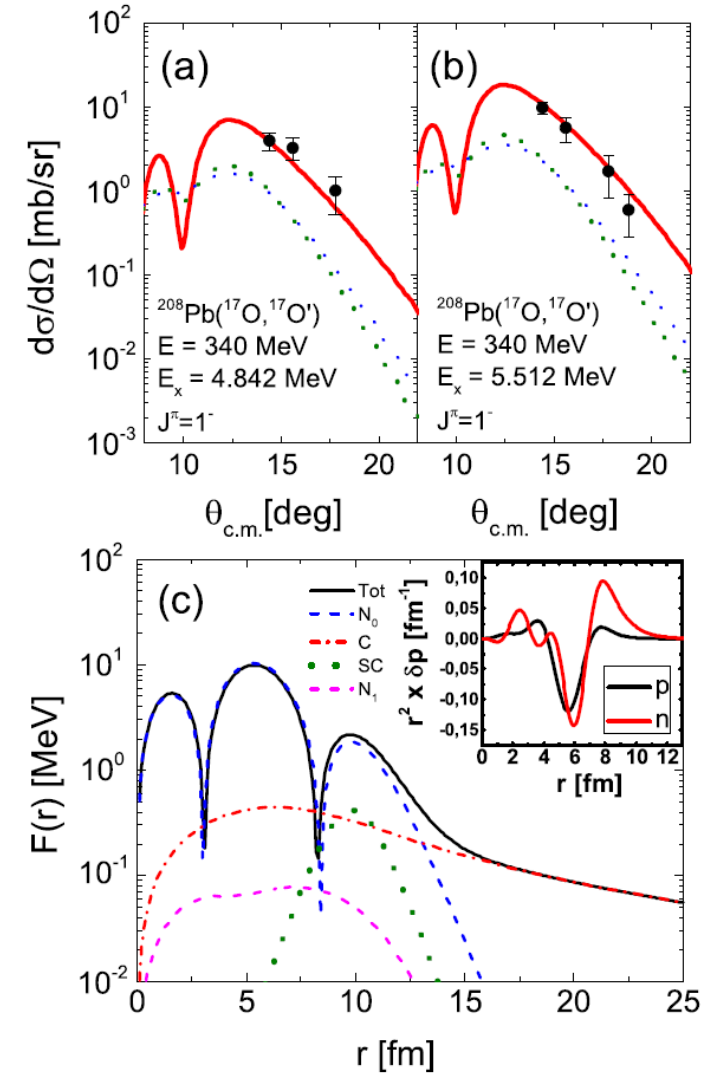
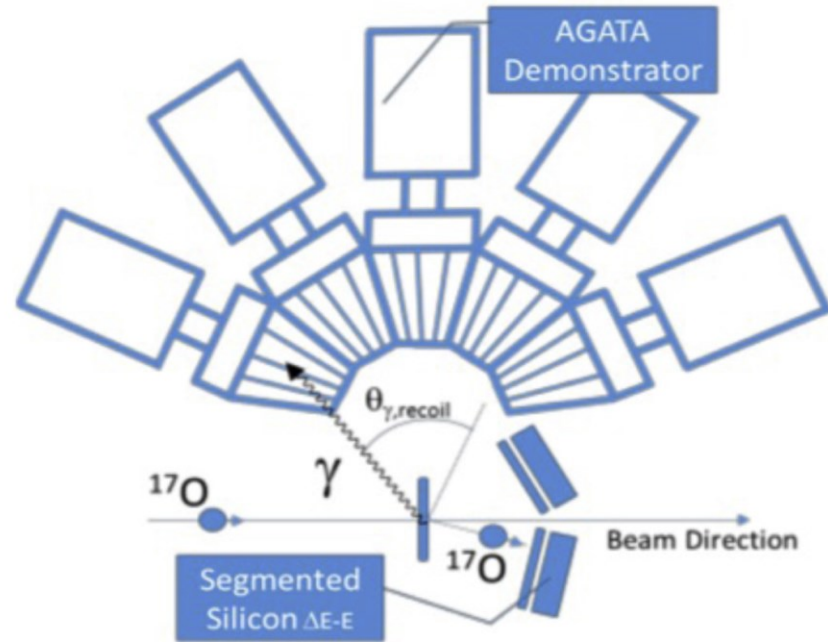
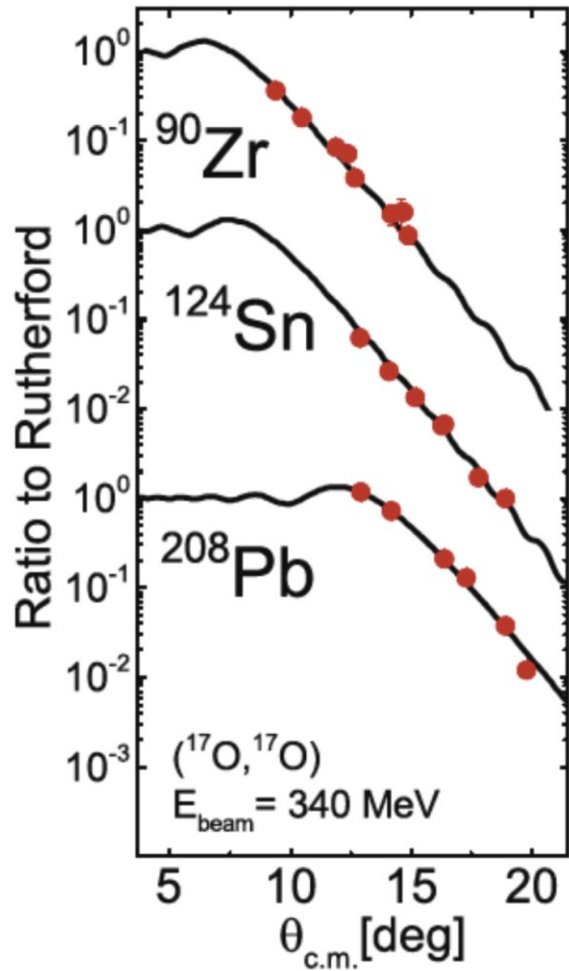


Escape lines are identified and discriminated by γ -ray tracking

First interaction points yield angular distributions:

- E1 transition from the 1^- state at 5.512 MeV
- E2 transition from the 2^+ state at 6.194 MeV

Structure of the Pygmy Dipole Resonance



S. Ceruti et al., Phys. Rev. Lett. 115, 222502 (2015)

L. Pellegrini et al., Phys. Lett. B **738**, 519 (2014).

F. Crespi, et al., Phys. Rev. Lett. **113**, 012501 (2014)

Isospin dependence of transition strengths

FRS-AGATA-LYCCA setup @ GSI

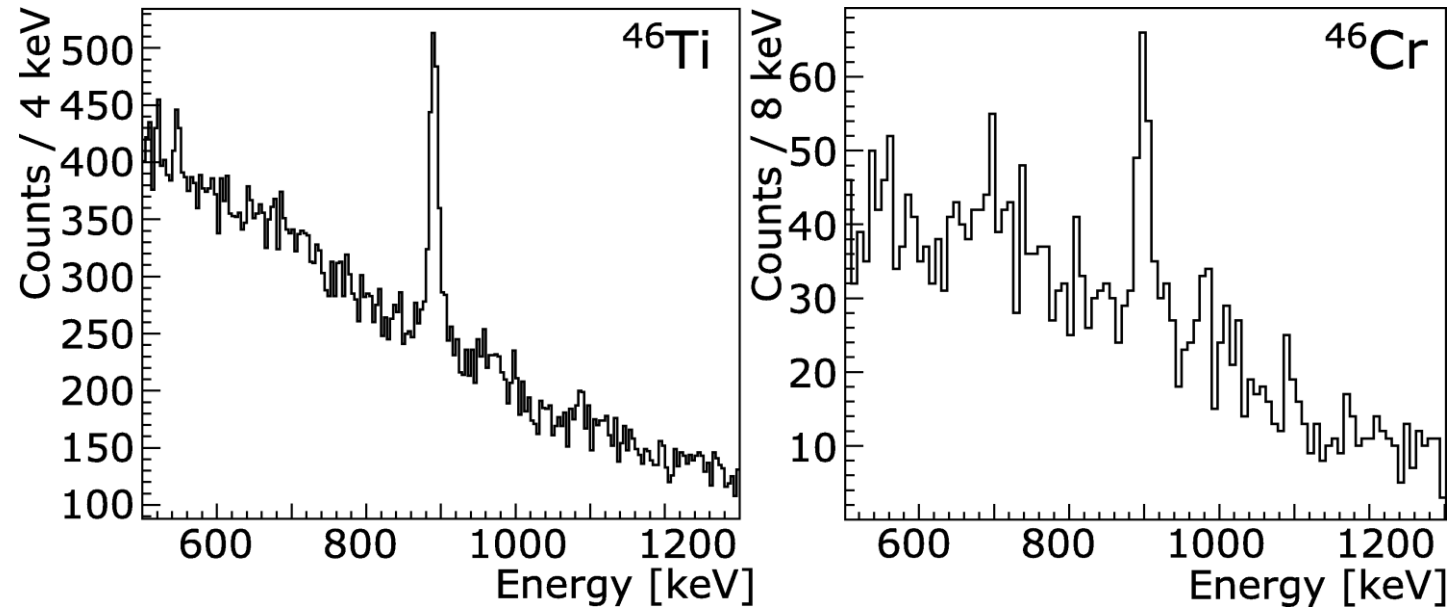
primary ^{58}Ni beam, 600 MeV/A

three secondary beams ^{46}Cr , ^{46}V and ^{46}Ti

beam energies: 180, 176 and 178 MeV/A

Two different methods for $0^+_{g.s.} \rightarrow 2^+_1$ $B(E2)$ strength

(i) Relativistic Coulomb excitation (Au target 500 mg/cm 2 , $v/c \approx 0.53$)



Doppler shift at $v/c \approx 0.53$ up to 60%

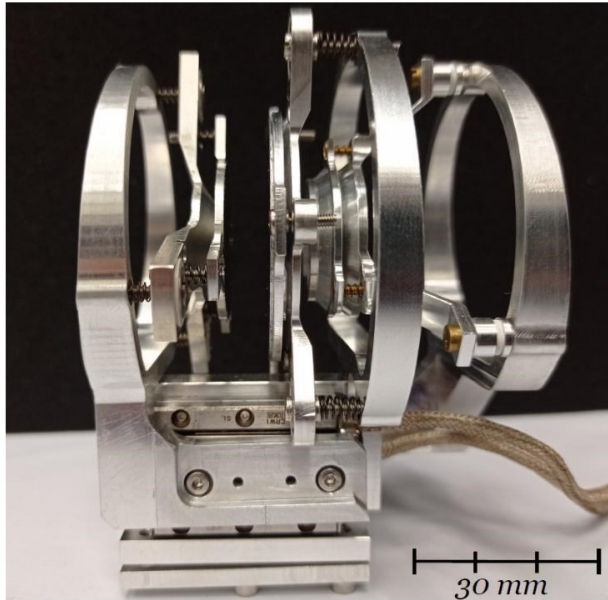
Energy resolution of $0^+_{g.s.} \rightarrow 2^+_1$ transition ($\Delta E \approx 1.7\%$)

fits theoretical limit

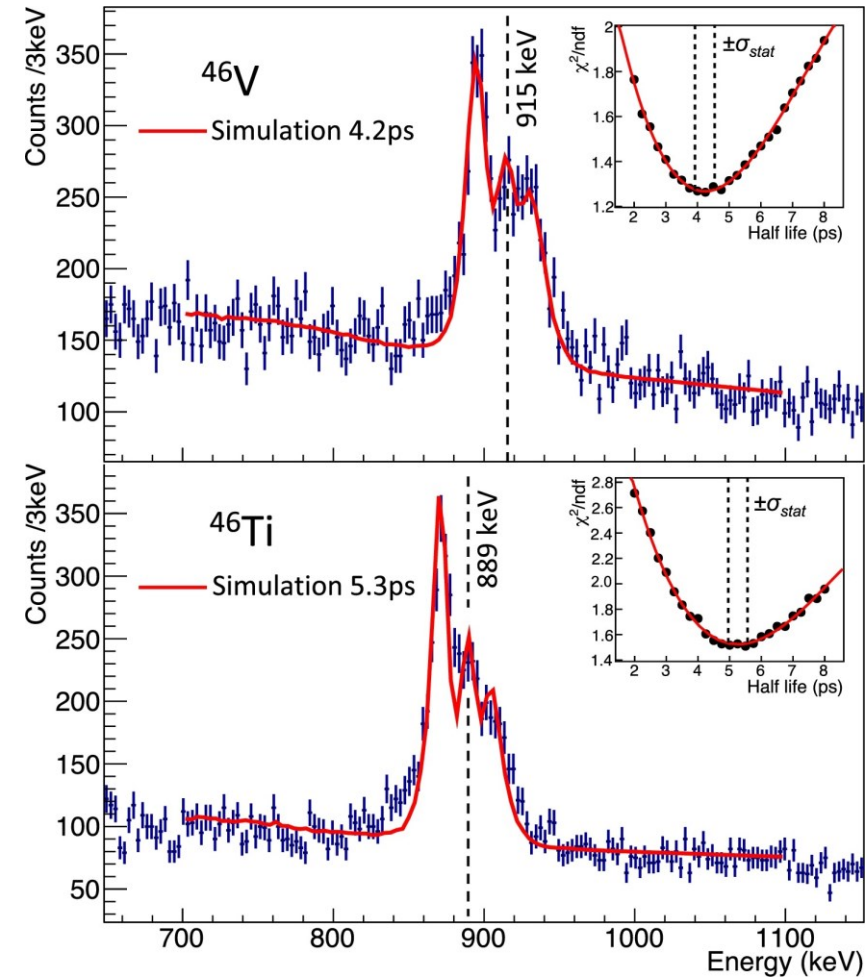
A. Boso, et al., Phys. Lett. B 797 (2019) 134835.

Isospin dependence of transition strengths

Two different methods for $0^+_{g.s.} \rightarrow 2^+_1$ $B(E2)$ strength
(ii) Differential three foil plunger Au (750 +500 +500) mg/cm²
line shape with three peaks $v/c = 0.527, 0.509, 0.488$

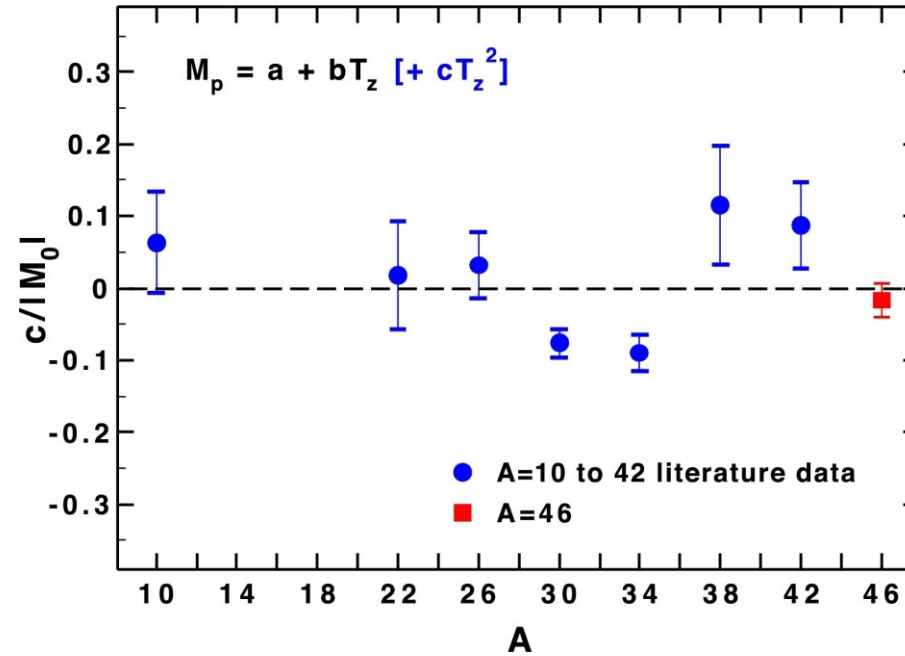
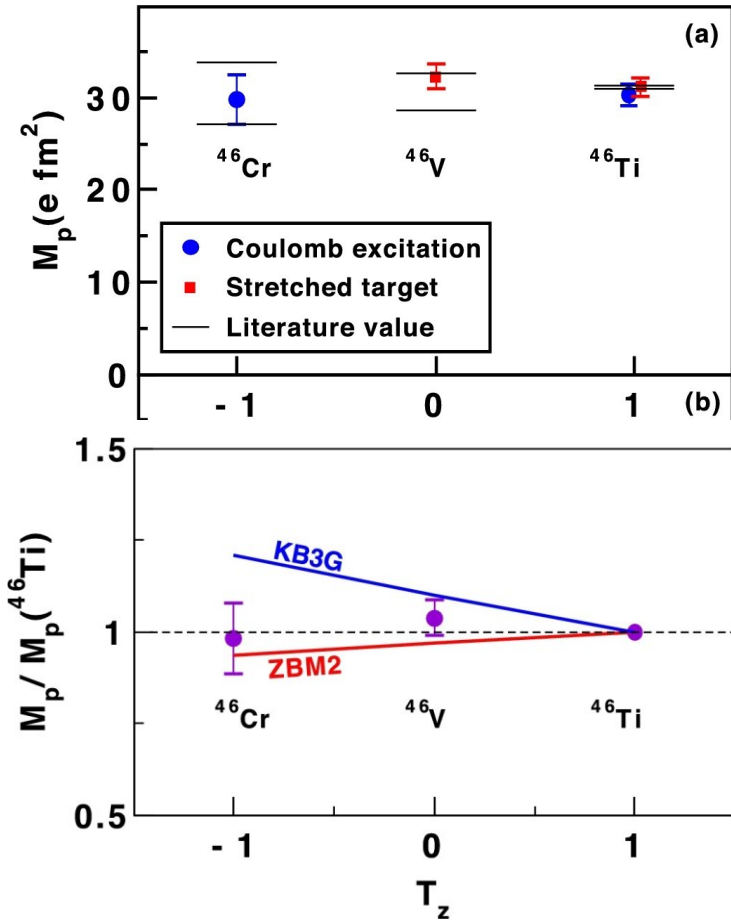


Cologne Compact Differential Plunger
M. Beckers, et al., NIM A 1042 (2022) 167418



A. Boso, et al., Phys. Lett. B 797 (2019) 134835.

Isospin dependence of transition strengths



Isospin dependence of the proton matrix element $M_p(T_z)$ for electromagnetic transitions of $T=1$ triplet:

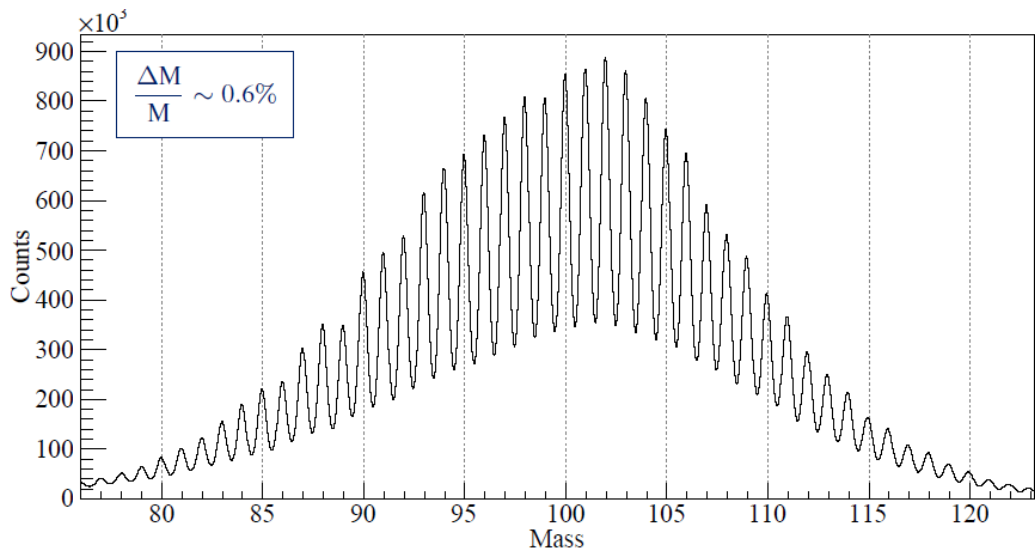
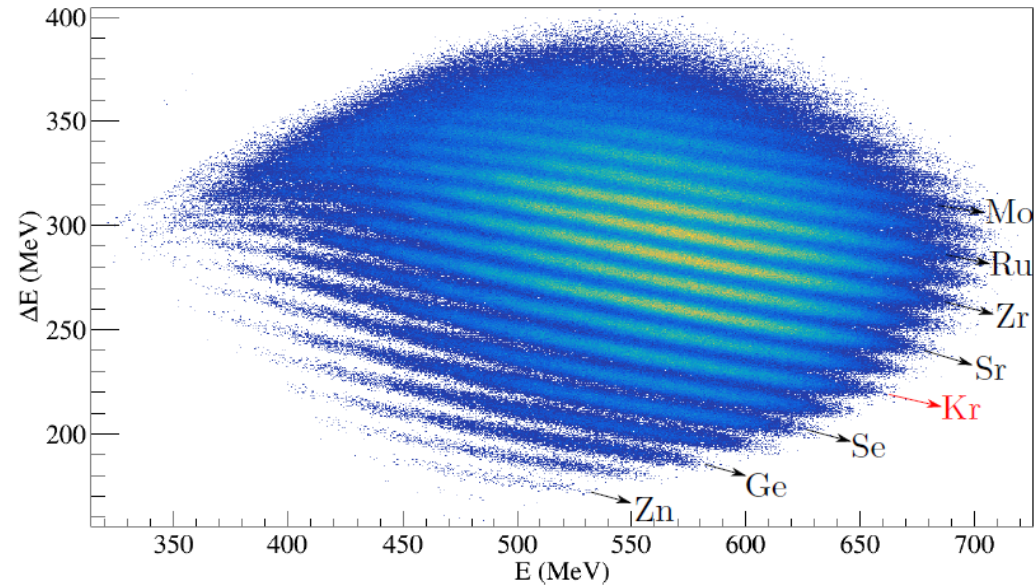
$$M_p(T_z) = 1 + \frac{1}{2} [M_0 - T_z M_1^{T_z=1}]$$

M_0 isoscalar matrix element $62.2(15) \text{ efm}^2$,

$M_1^{T_z=1}$ isovector matrix element $0.0(15) \text{ efm}^2$.

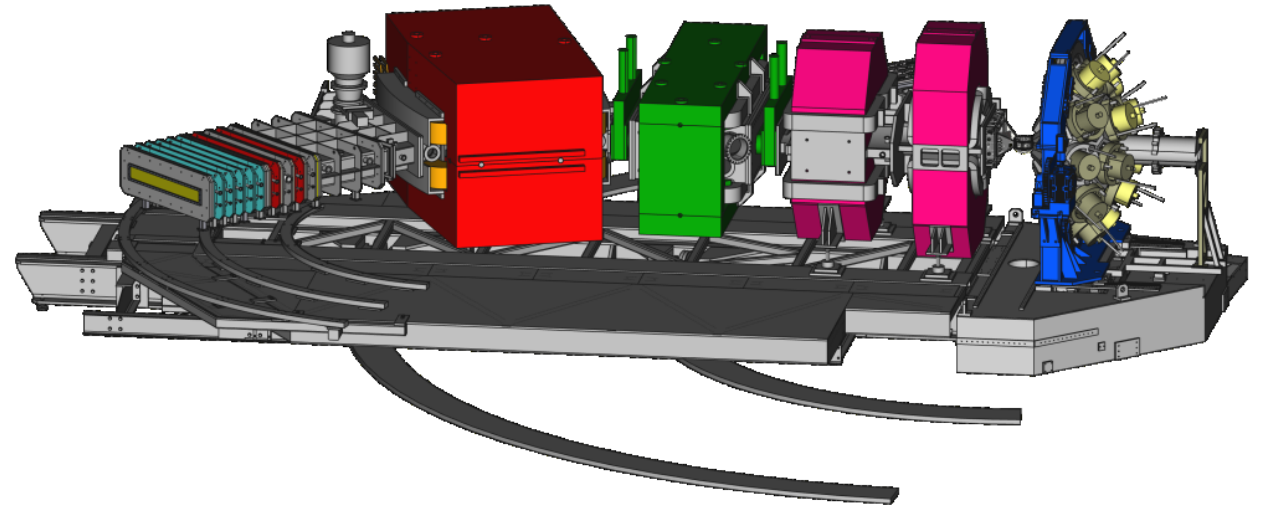
In the limit of pure isospin, the analogue proton matrix elements should be exactly linear with T_z .

The GANIL Campaign [2015-2021]



45 AGATA detectors on-line Coupled to VAMOS spectrometer

E. Clément et al.; NIM A 855, 1-12 (2017)



J. Dudouet, et al.; Phys. Rev. Lett. 118, 162501 (2017)

C. Delafosse, et al.; Phys. Rev. Lett. 121, 192502 (2018)

D. Ralet, et al.; Phys. Lett. B 797, (2019) 134797

B. Cederwall, et al.; Phys. Rev. Lett. 124, 062501 (2020)

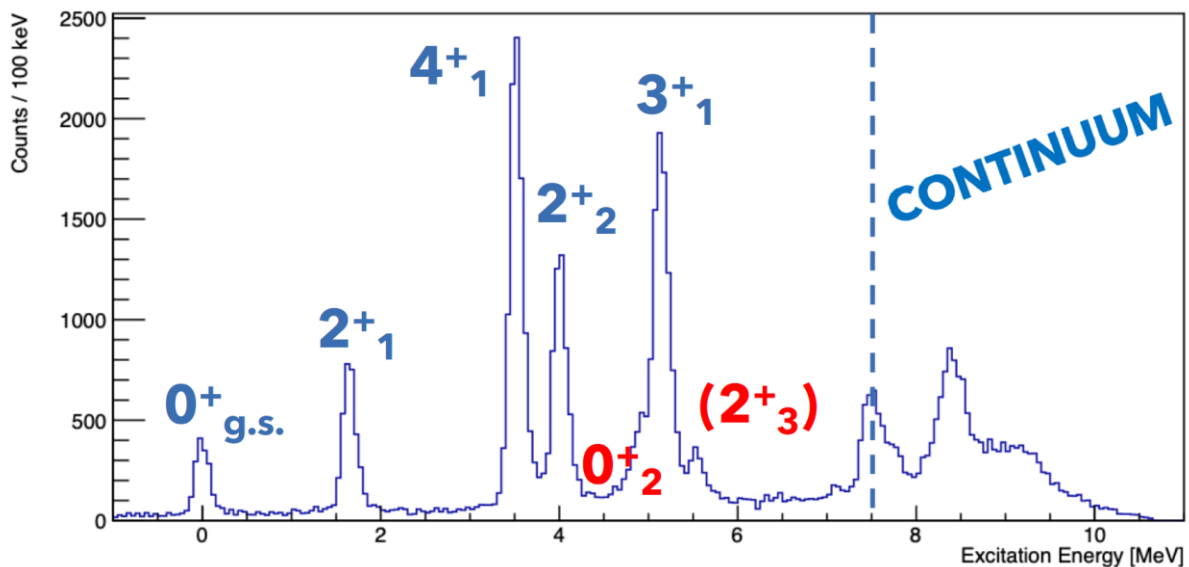
M. Siciliano, et al.; Phys. Lett. B 806 (2020) 135474

R. M. Pérez-Vidal, et al.; Phys. Rev. Lett. 129, 112501 (2022)

I. Zanon, et al.; Phys. Rev. Lett. 131, 262501 (2023)

Ch. Fougères, et al.; Nature Communications (2023) 14:4536

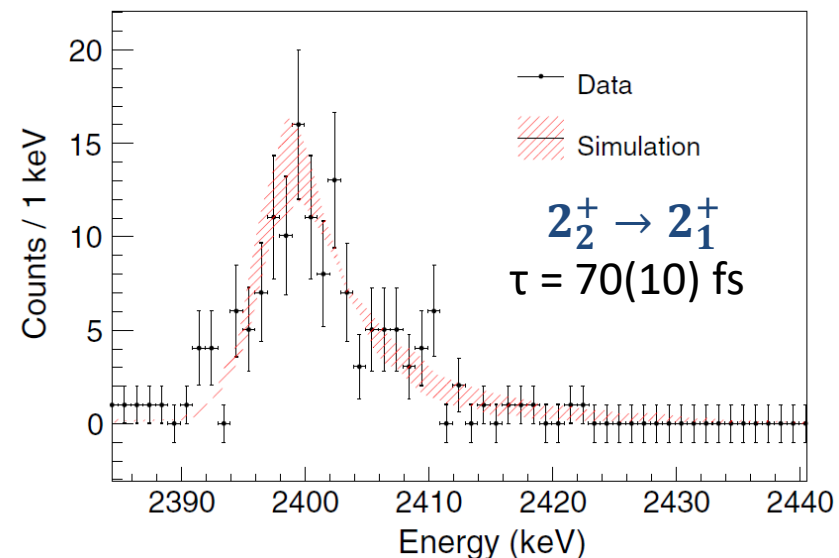
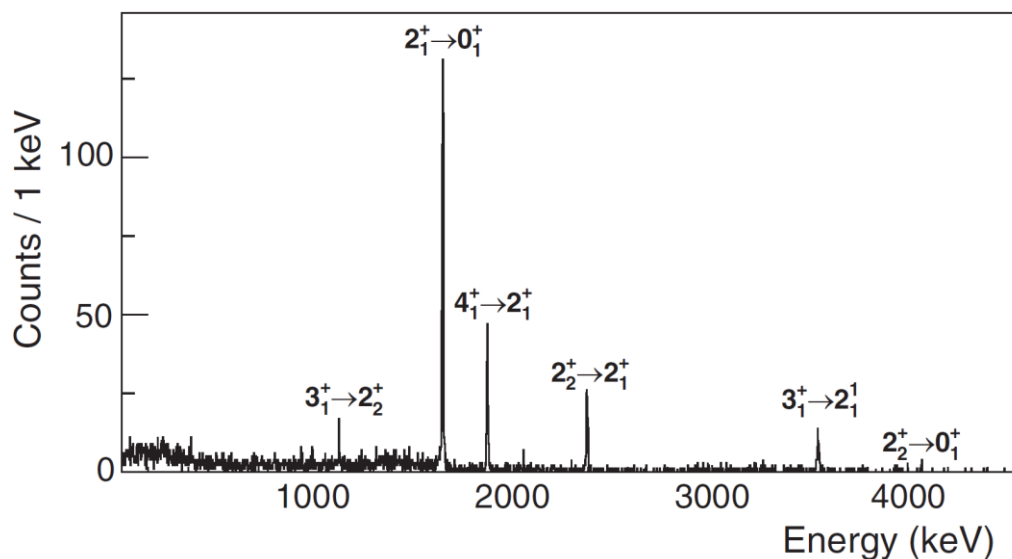
High-Precision Spectroscopy of ^{20}O



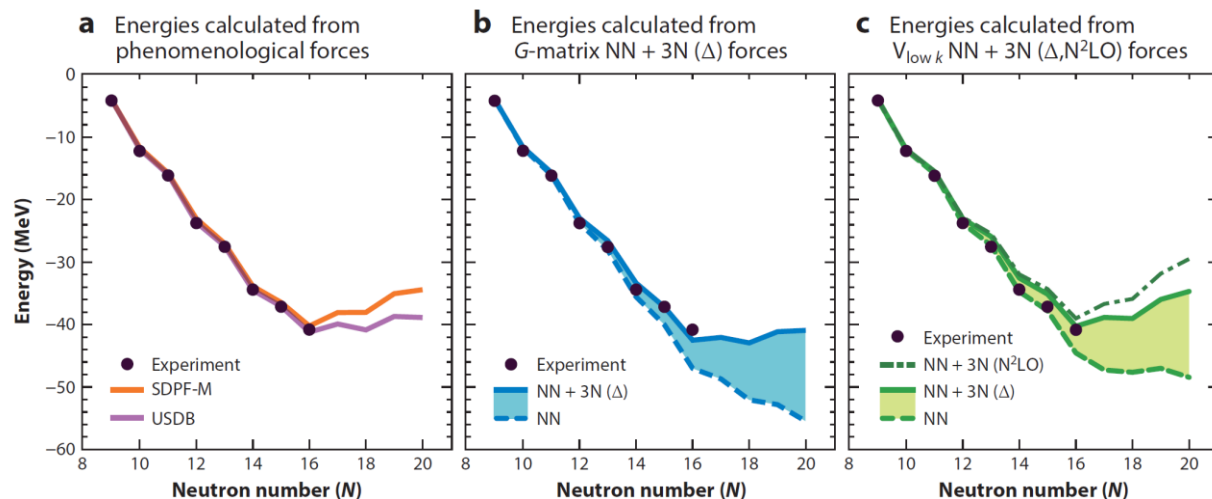
- SPIRAL1 accelerator @ GANIL
- **Radioactive ^{19}O beam, 8 MeV/A, 4×10^5 pps**
- Target CD_2 0.3 mg/cm² (+ Au 24.4 mg/cm²)
- $^{19}\text{O}(d,p)^{20}\text{O}$ direct reaction, inverse kinematics
- AGATA + MUGAST + VAMOS.

Efficiency, energy resolution, position resolution,
Doppler correction capability

➔ Doppler shift attenuation method



High-Precision Spectroscopy of ^{20}O



Chiral Effective Field Theory

Position of the drip line of oxygen isotopic chain is reproduced by introducing **3N forces**.

*K. Hebeler, J.D. Holt, J. Menendez, A. Schwenk
Annu. Rev. Nucl. Part. Sci. (2015) 65:457-484*

USDB

B.A. Brown, W.A. Richter,
Phys. Rev. C 74, 034315 (2006)

N³LO_{lnl}

V. Soma, et al. Phys. Rev. C 101, 014318 (2020)

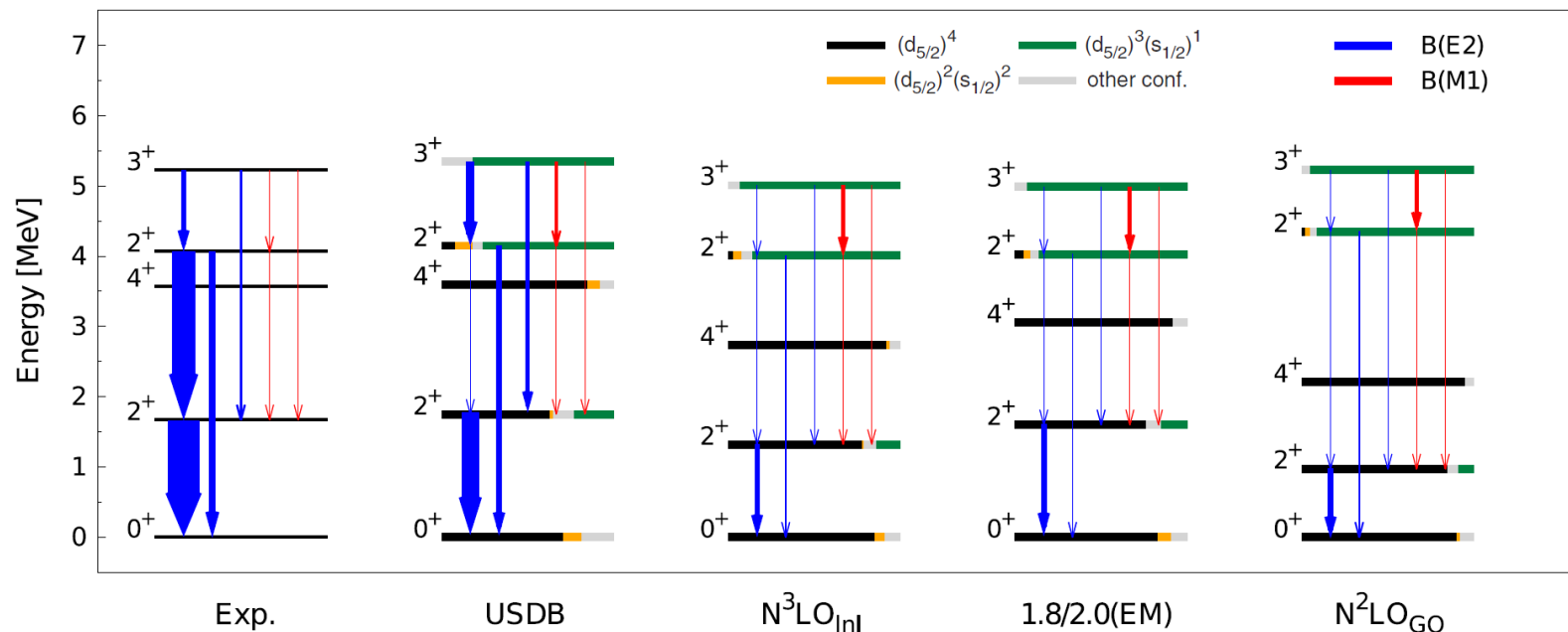
1.8/2.0(EM)

K. Hebeler, et al. Phys. Rev. C 83, 031301(R) (2011)

J. Simonis, et al. Phys. Rev. C 96, 014303 (2017)

N²LO_{GO}

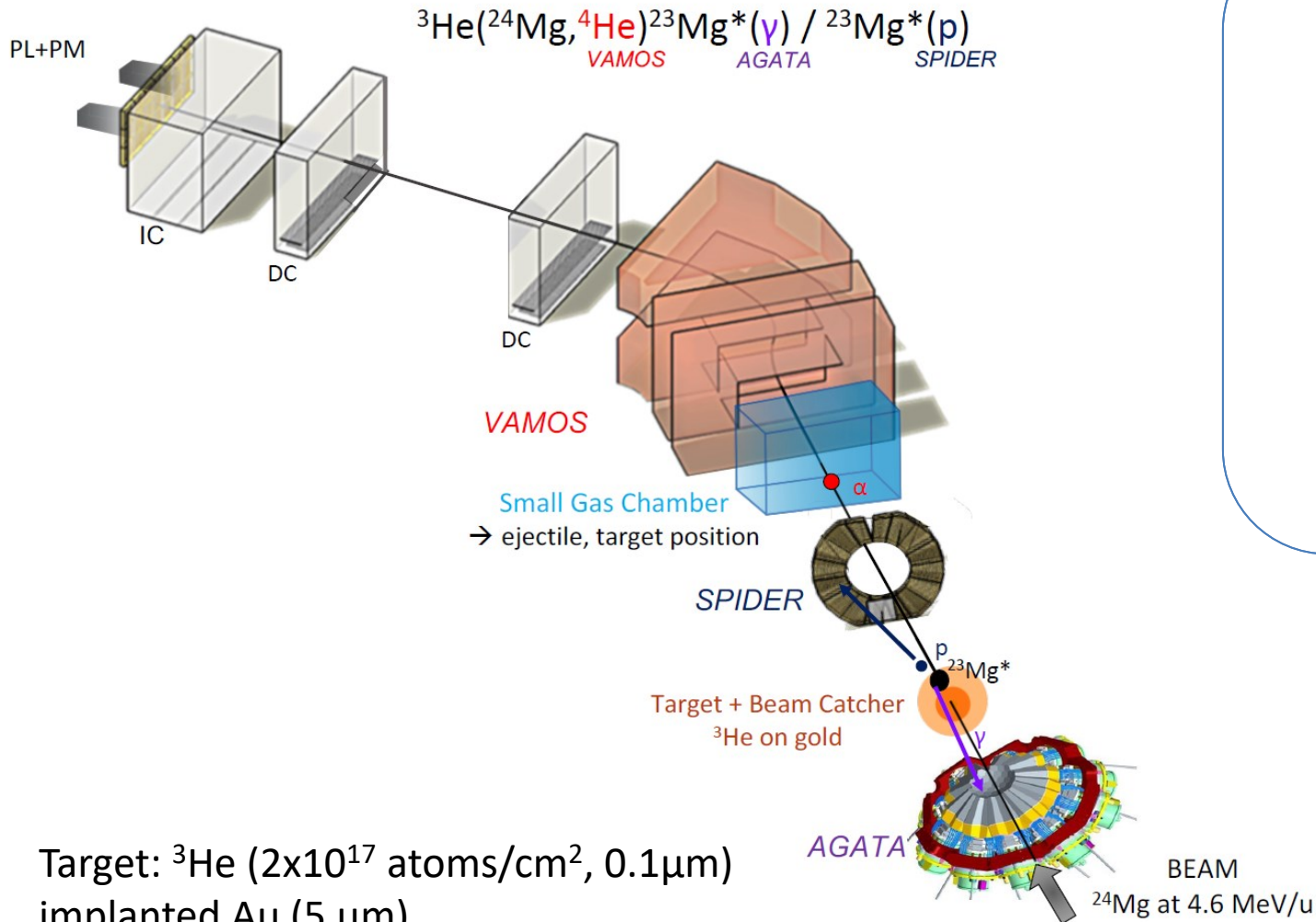
W. G. Jiang, et al. Phys. Rev. C 102, 054301 (2020).



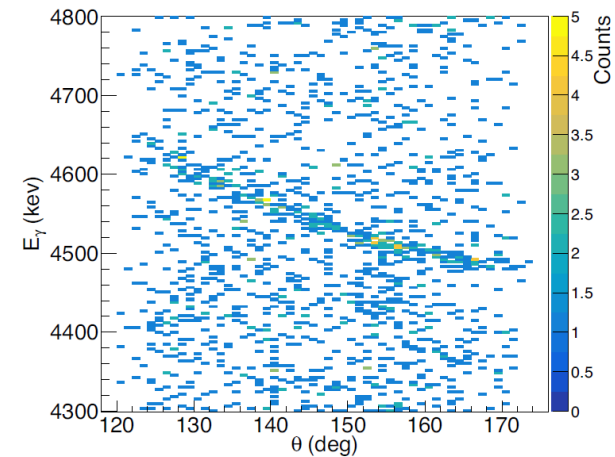
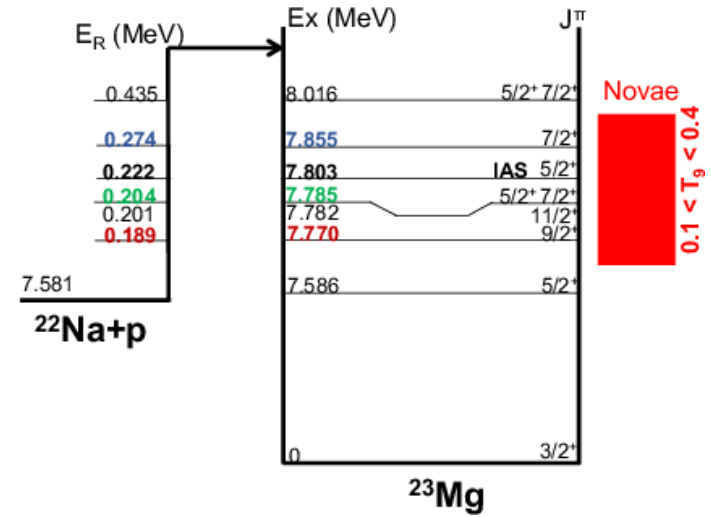
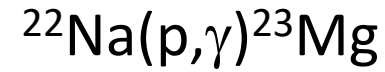
I. Zanon, et al.; Phys. Rev. Lett. 131, 262501 (2023)



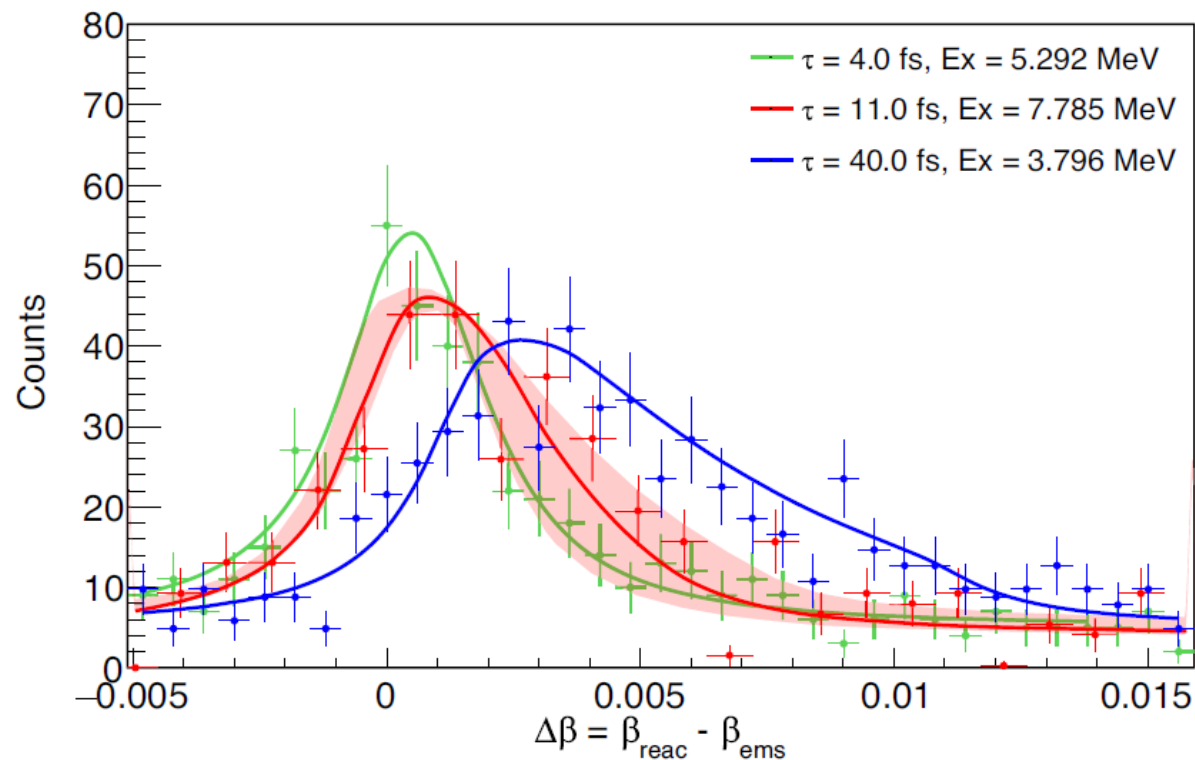
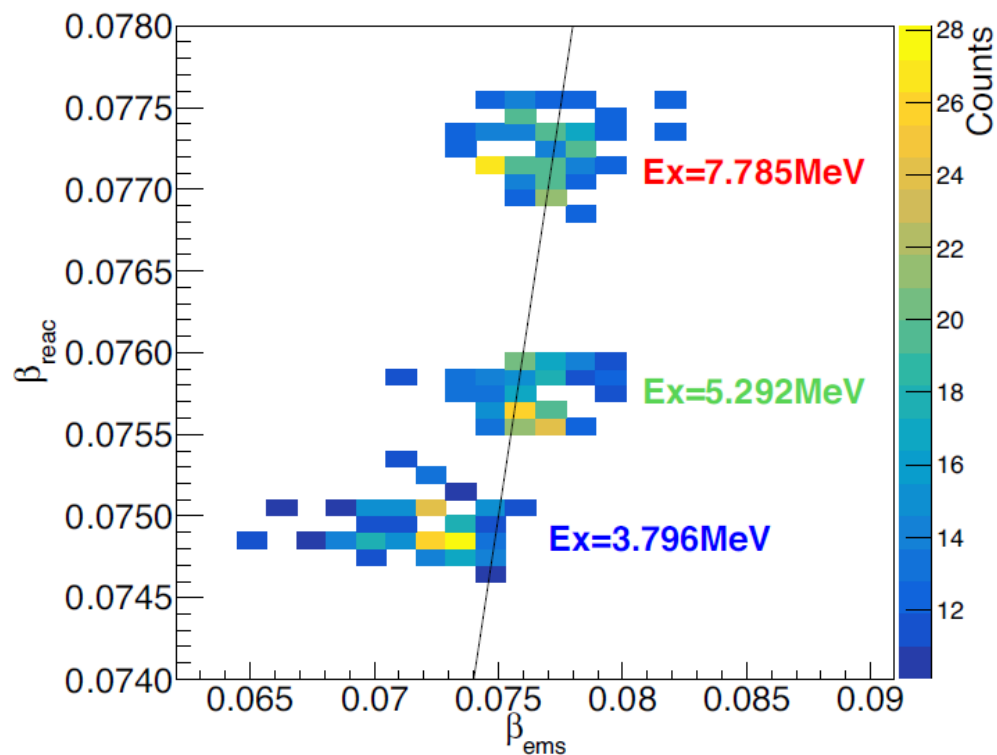
Measuring femtosecond nuclear lifetimes



Target: ${}^3\text{He}$ (2×10^{17} atoms/cm², 0.1 μm)
 implanted Au (5 μm)
 Stopping time of ${}^{23}\text{Mg}$ in Au: 500 fs



Measuring femtosecond nuclear lifetimes



Novel method: velocity difference $\Delta\beta$

β_{reac} velocity at time of the reaction from ^4He ejectile

β_{ems} velocity at time of γ -ray emission

Deceleration of ^{23}Mg ions is for short lifetimes ($\tau \lesssim 100 \text{ fs}$) almost constant ($dE/dx \approx \text{constant}$), $\Delta\beta \propto \Delta t$, right side tail of the curves follows exponential decay function

β_{ems} from
Doppler shift
 ΔE_γ , $\Delta\theta$

$$R = E_\gamma / E_{\gamma,0}$$

$$E_\gamma = E_{\gamma,0} \frac{\sqrt{1 - \beta_{\text{ems}}^2}}{1 - \beta_{\text{ems}} \cos(\theta)}$$

$$\beta_{\text{ems}} = \frac{R^2 \cos(\theta) + \sqrt{1 + R^2 \cos^2(\theta) - R^2}}{R^2 \cos^2(\theta) + 1}$$

Measuring femtosecond nuclear lifetimes

Lifetime of astrophysical state at 7.333MeV: $\tau = 11_{-5}^{+7}$ fs

reduced magnetic dipole transition probability: $B(M1) = 0.017_{-0.008}^{+0.011} \mu_N^2$

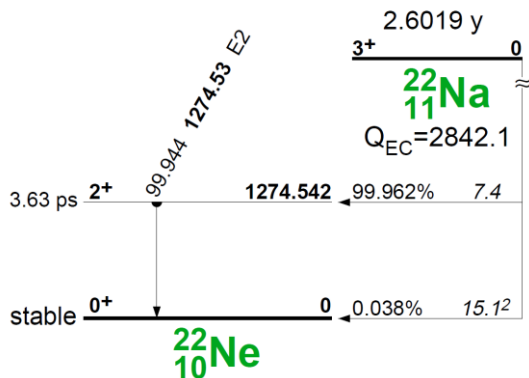
Proton branching ratio: BRp = 0.68(17)%

Resonance strength: $\omega\gamma = 0.24_{-0.04}^{+0.11}$ meV

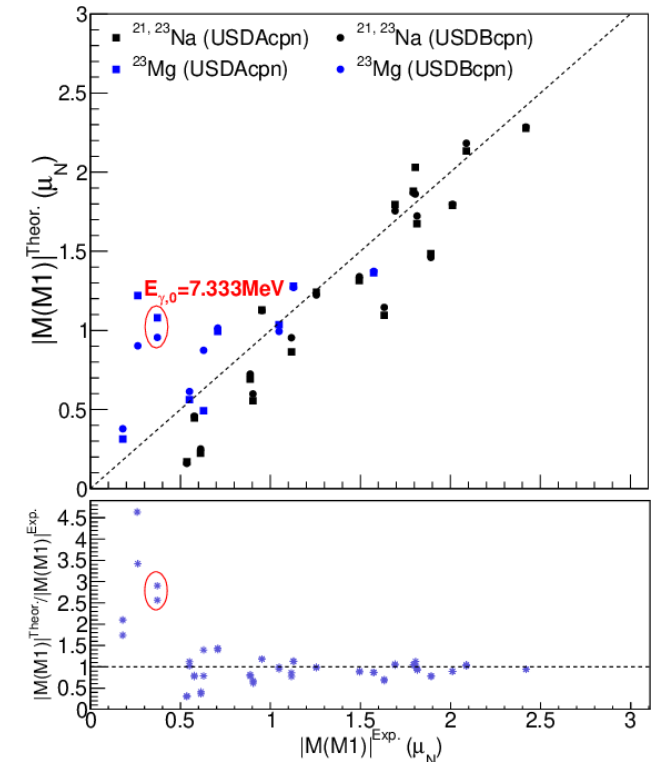
Nova models:

Temperature $T_{\text{base}} \sim 5 \times 10^7$ K, reaction chain: $^{20}\text{Ne}(p, \gamma)^{21}\text{Na}(\beta^+)^{21}\text{Ne}(p, \gamma)^{22}\text{Na}$
 rapid rise in the ^{22}Na abundance.

higher temperature $T_{\text{base}} \sim 5 \times 10^8$ K, reaction $^{22}\text{Na}(p, \gamma)^{23}\text{Mg}$ destruction of ^{22}Na



- Predictions of the 1.275 MeV γ -ray flux emitted from a nova.
- Estimates of the maximum detectability distance of novae in γ rays, via 1.275 MeV line.
- Expected sensitivities of e-ASTROGRAM (3×10^{-6} photons $\text{cm}^{-2} \text{s}^{-1}$) and COSI (1.7×10^{-6} photons $\text{cm}^{-2} \text{s}^{-1}$)

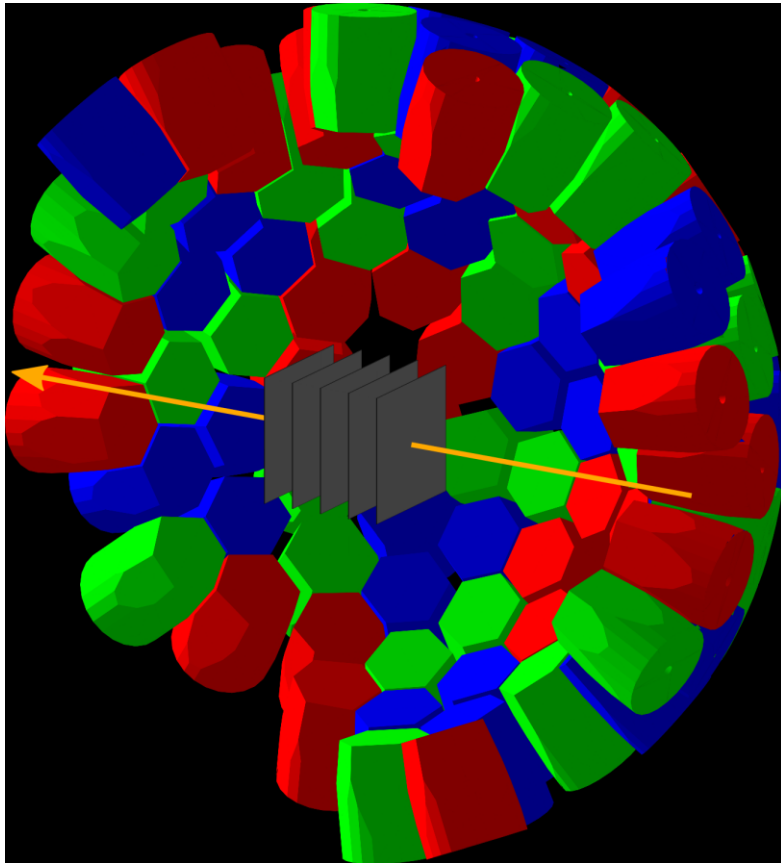


LISA: Lifetime measurements with Solid Active targets

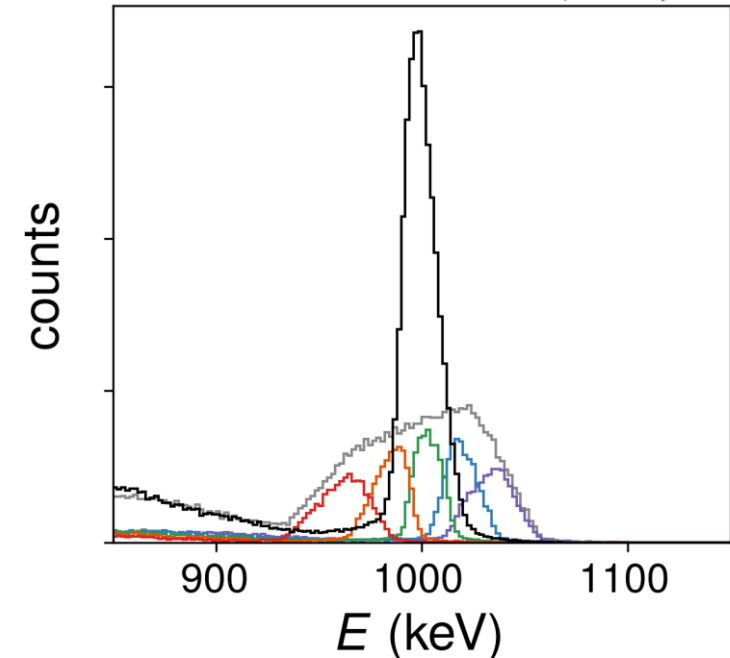
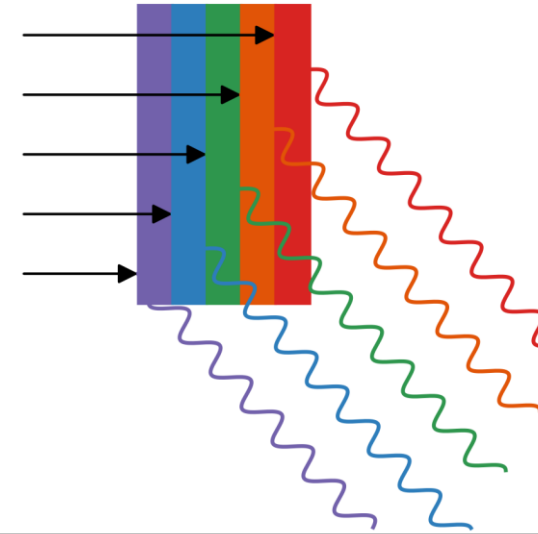
- Energy resolution determined by unknown velocity in the target
- Several layers of active targets
- Event-by-event determination of reaction position $\rightarrow (\beta, z)$

Opens new possibilities for lifetime measurements using AGATA at FAIR:

- Evolution of collectivity in Islands of Inversion
- Fate of the N=82 and 126 shell closures
- And many more



Compact array of active target detectors inside AGATA



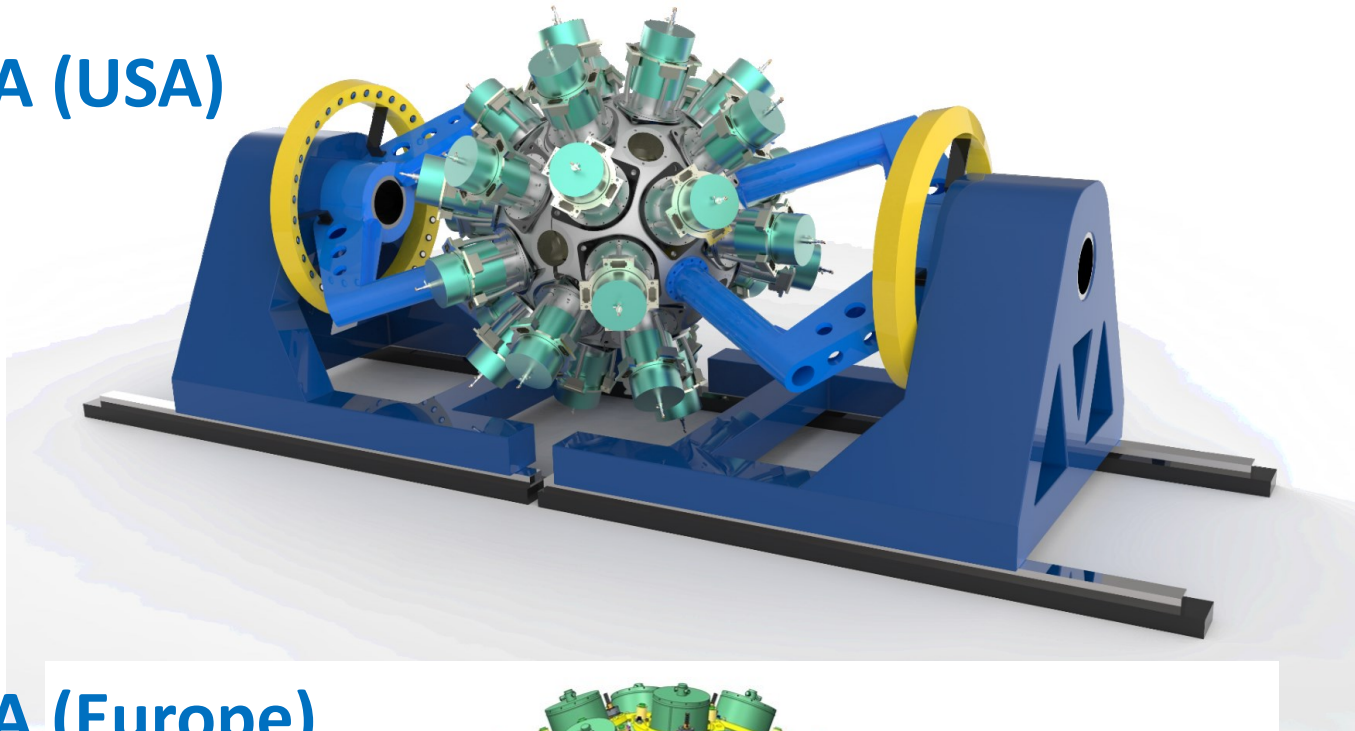
Courtesy K. Wimmer, GSI



European Research Council
Established by the European Commission

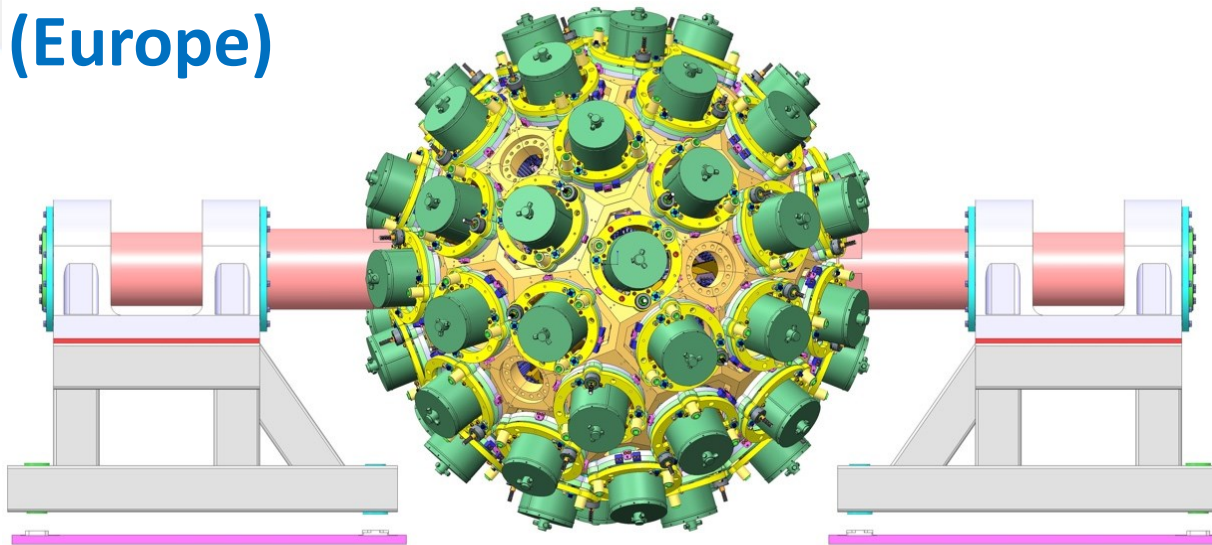
Gamma-Ray Energy Tracking Arrays

GRETA (USA)



- 120 Ge crystals
- 30 Quad “modules”
- main user FRIB
- final completion 2025

AGATA (Europe)



- 180 Ge crystals
- 60 Triple “clusters”
- MoU Phase 2
- 45 Triple “clusters”
- 3π completion 2032

Summary

- **Status AGATA**
 - ✓ > 60 detectors, digital electronics, PSA, γ -ray tracking
 - ✓ position sensitivity (E,x,y,z,t) ΔE , Δx , Δt
- Major improvements for in-beam γ -ray spectroscopy
- Ongoing AGATA campaigns continuously produce excellent physics results
- **Promising perspectives** for future experiments with RIBs at FAIR, SPES, SPIRAL2, ...
- New MoU to complete the 3π AGATA configuration
- Topical Collection on AGATA, EPJ A special issue (2024)
A.Bracco, G.Duchêne, Zs.Podolyák, PR, Prog. Part. Nucl. Phys. 121 (2021) 103887

